Journal of King Saud University – Engineering Sciences 32 (2020) 351–359

Contents lists available at ScienceDirect

Journal of King Saud University – Engineering Sciences

journal homepage: www.sciencedirect.com

Original article

Basic-dye adsorption in albedo residue: Effect of pH, contact time, temperature, dye concentration, biomass dosage, rotation and ionic strength

Carlos Eduardo de Farias Silva [a,c,*], Brígida Maria Villar da Gama [a,b], Andreza Heloiza da Silva Gonçalves [c], Josimayra Almeida Medeiros [a], Ana Karla de Souza Abud [d]

[a] Center of Technology, Federal University of Alagoas, Campus A. C. Simões, 57072-970 Maceió, AL, Brazil
[b] Center of Technology and Geosciences, Federal University of Pernambuco, Recife, PE, Brazil
[c] Institute of Chemistry and Biotechnology, Federal University of Alagoas, Campus A. C. Simões, Maceió, AL, Brazil
[d] Food Technology Department, Federal University of Sergipe, São Cristóvão, SE, Brazil

ARTICLE INFO

Article history:
Received 10 August 2018
Accepted 25 April 2019
Available online 30 April 2019

Keywords:
Orange albedo
Cationic dye
Biosorbent
Performance
Methylene blue
Salinity

ABSTRACT

This work was aimed at evaluating the efficiency of orange albedo as an adsorbent for the removal of cationic dyes in aqueous solution. The material was characterised by SEM, FTIR and pH_Z. In order to verify the influence of the main parameters essential for adsorption, kinetic, equilibrium and thermodynamic studies were carried out, as well as a study regarding the influence of rotation and salinity (ionic strength). For SEM, the material presented a heterogeneous and porous surface, while the FTIR spectra identified bands assigned to hydroxyl and carboxyl groups and a pH_Z of 4.61, usually associated to the adsorption on biomass, making it possible to use solutions at the natural pH. The equilibrium was reached at approximately 10 min, with no significant differences between the kinetic models. The best condition in terms of biosorbent saturation was found when 1% of biomass, 100 rpm and 30 °C were applied reaching an experimental q of 70 mg g^{-1} for 1000 mg L^{-1}. The isothermal model with better adjustment to the experimental data was the Langmuir-Freundlich model, with a q_{max} of 77.79 mg g^{-1} at 30 °C. The thermodynamic values demonstrated a spontaneous nature of the process. In terms of the salinity (ionic strength) influence, it could be observed that the adsorptive capacity was reduced in between 20 and 65% when C_{NaCl} varied between 0.1 and 1% (w/v). These results therefore demonstrate the technical potential of orange albedo as an adsorbent, mainly when any activation process is used.

1. Introduction

In 2017, Brazil obtained a record harvest of fruit, totalling R$ 38.9 billion among the 23 fruit products surveyed by the IBGE, an increase of 4.6% in relation to 2016, especially orange, with 2% more than the previous year 2017, ranked as the third largest producer of fruits in the world, only behind China and India (IBGE 2018).

Some 50% of the Brazilian production of fruits is transformed in fruit, pulp, jam, etc., to supply the national market at long distances and in-between the post-crop periods. However, these transformation processes in Brazil usually lead to a great residues production, commonly used as animal fodder (ABF 2013) or, in some more urban scenarios, with these residues being released in landfills or even in the environment, due to the unavailability of suitable infrastructures to meet the great demand of biomass and/or lack of commercial use for those, with great negative impact to the environment (Babbar and Oberoi 2014).

Ranging from about 50 to 70% (w/w) of processed fruits and with high concentrations of organic compounds, the citrus peel waste has a significant annual world production, leading to considerable constraints for their management due to economic and environmental factors. To minimize the management costs and prevent environmental damages, waste recovery methods are being sought to contribute to the growth of the bioeconomy and

* Corresponding author at: Center of Technology, Federal University of Alagoas, Campus A. C. Simões, 57072-970 Maceió, AL, Brazil.
E-mail address: eduardo.farias.ufal@gmail.com (Carlos Eduardo de Farias Silva).
Peer review under responsibility of King Saud University.

Production and hosting by Elsevier

https://doi.org/10.1016/j.jksues.2019.04.006
1018-3639/

mitigate the negative environmental effects related to the agroindustry, generating products focused at the energy, food, cosmetics and pharmaceutical industries (Sharma et al., 2017; Zema et al., 2018).

Proved to be one of the promising approaches to remove pollutants from environmental waters or sewage, many researchers are exploring the adsorption potential of non-conventional, naturally-occurring agricultural residues due to their low cost, environmental friendliness, local availability and sustainability (Daud et al., 2018). Originated from plant materials, these residues mainly consist of cellulose, lignin and hemicellulose molecules, exhibiting fibrous properties and forming complex matrices, which results in better adsorption properties (Zhao et al., 2017).

Although adsorption using activated carbon has been widely investigated for the removal of contaminants, the production costs of this material are high, with its use not complying with its applicability in controlling pollution. Therefore, the search for alternative adsorbents has continuously been a matter of further investigation (Kumar et al., 2014).

According to Yagub et al. (2012) and Saini et al. (2018), approximately 100 tonnes of dyes per year are discharged in watercourses. Generated by textile, paper mills and dyeing industries, these effluents interrupt the photosynthetic activity in aquatic system and retards growth of the biotic community, tuning water unsuitable for consumption.

Due to the low cost and availability, several studies are being developed using agricultural residues for the removal of dyes as citrus (Asgher and Bhatti, 2012), mango seeds (Kumar et al., 2014), potato skin (Sharma et al., 2014), banana skin (Moubarak et al., 2014), coconut shell (Etim et al., 2016) and tomato seeds biomasses (Najafi et al., 2016). However, none of these studies were found to solely use citrus albedo as an adsorbent of cationic dyes, which makes it interesting to investigate the properties of this residue better, especially given the importance of obtaining value added products (e.g. essential oil) from the bark of this biomass.

Various aspects must be taken into account for the dye/adsorbent interaction study, namely the chemical structure of the biomass and the characteristics of textile effluents (Aksu, 2005; Silva et al., 2016). Due to this, the most significant variables of the adsorption process, such as pH, temperature, contaminant content, rotation, biomass concentration, ionic strength (salinity), among others, should be evaluated.

Used for dyeing cotton, wool, silk, leather, paper, cosmetic, pharmaceutical, tannery and food processing industries, methylene blue is widely applied as a "model" compound to represent the adsorption behavior of toxic chemicals, particularly organic dyes, onto carbon materials (Wang et al., 2018; Saini et al., 2018).

Thus, this work was aimed at characterising the adsorption of a cationic dye (methylene blue) using orange albedo residue from sweet orange as an adsorbent. The variables pH, biomass concentration, dye content, temperature, rotation and kinetic studies were analysed in order to optimise its applicability on effluent treatment.

2. Methodology

2.1. Preparation and characterisation of orange albedo

The oranges used in this study were collected from of Santana do Mandaú, in the Brazilian State of Alagoas, Brazil. The fruits were initially peeled and squashed, in order to obtain the juice, and the residues were cut and disinfected in sodium hypochlorite solution (100 mg L^{-1}) for 15 min. After being rinsed, the material was placed in an air-circulation furnace at 50 °C under constant weight and the dry material was crushed with a Wylle (30 mesh) cutting mill and packed in hermetically plastic flasks at room temperature.

The physicochemical properties of the adsorbent were characterised using the following techniques: scanning electron microscope (SEM, Shimadzu SSX-550), which analysed the physical morphology of the albedo's surface; Fourier transform infrared spectroscopy (FTIR), for identifying the functional groups present in the adsorbent in the band of 400–3500 cm^{-1}, as well as the pH at the point of zero charge (pH_Z). The pHz was determined according to the methodology described by Silva et al. (2016), using the graphical method of 11 points, at a range of solution pH between 2 and 11 adjusted with H_2SO_4 20% and NaOH 40% with 1% of biomass load (w/v) and 100 rpm at 30 °C for 60 min of contact time. After the adsorption process, centrifugation was performed to remove the solid phase and the liquid phase analysed by UV–vis spectrophotometer at 653 nm using a calibration curve of methylene blue as standard.

2.2. Dye concentrations

The cationic dye used in the adsorption trials was methylene blue (Sigma®), suitable as a model for cationic dyes removal from aqueous solutions (Liu et al. 2012). A stock solution of 1,000 mg L^{-1} of methylene blue (MB) was initially prepared and subsequently diluted to prepare 50, 100, 250, 350, 500, 750 and 850 mg L^{-1} solutions, used in the adsorption studies. Adsorption capacity was calculated by Eq. (1), with q being the adsorptive capacity (mg g^{-1}), C_0 the initial concentration, C_f the concentration at (final) equilibrium (mg L^{-1}), V the volume of the solution (L) and S the mass of adsorbent (g).

$$q = \frac{(C_0 - C_f)V}{S} \quad (1)$$

2.3. Effect of dye solution pH, biomass load and rotation

The influence of initial solution pH (natural pH just dissolving the dye in water) on the adsorptive capacity was subsequently evaluated to verify if during the adsorption process on time it changed significantly affecting the process with respect the pHz, with the biomass being in contact with solutions of 50–1,000 mg L^{-1} in their initial solution pH range, under constant stirring of 100 rpm for 60 min using 1% of biomass (w/v), in a rotating incubator (TE-424, TECNAL) at 30 °C. The pH was measured using a glass-electrode digital pH meter (PHS-3B PHTEK), previously set with buffer solutions at a pH of 4 and 7.

Then, considering the adequate pH range, the influence of biomass dosage was evaluated at a range of 10–30 g L^{-1} (1–3% w/v). The trials were carried out using a range of dye concentration between 50 and 1,000 mg L^{-1} at 100 rpm and 30 °C for 60 min.

The stirring rate of the adsorbent/adsorbate system is considered to influence on the adsorption process, given the reduced resistance of the peripheral layer surrounding the adsorbent particle. When stirred, the particles of adsorbent and the molecules of adsorbate start moving in the solution, favouring the adsorption process (Mckay et al., 1980). For this reason, the study of the influence of rotation was performed for the rates of 60, 80 and 100 rpm, with biomass load of 1% (w/v) at 30 °C using a range of dye concentration between 50 and 1,000 mg L^{-1} in contact with the dye solution for 60 min.

2.4. Kinetic study

From the conditions established in previous experiments, the kinetic and thermodynamic equilibrium studies were developed. The kinetic study was carried out adding 1% (w/v) of adsorbent in MB solution with initial concentrations ranging from 50 to 1,000 mg L^{-1}. The contact times were of 0, 5, 10, 15, 20, 25, 30,

40, 50 and 60 min. Pseudo-first and pseudo-second order kinetic models were used, according to Eqs. (2) and (3) (Ho and Mckay, 1998; Ho and Mckay, 2000), respectively.

$$q_t = q_e\left(1 - e^{-k_1 t}\right) \tag{2}$$

$$q_t = \frac{q_e^2 k_2 t}{1 + q_e k_2 t} \tag{3}$$

where k_1 is the pseudo-first order kinetic rate constant (min^{-1}), q_e is the adsorptive capacity at equilibrium, q_t is the adsorptive capacity at time t ($mg\ g^{-1}$), t is the time (min) and k_2 is the pseudo-second order kinetic rate constant ($g\ mg^{-1}\ min^{-1}$).

2.5. Equilibrium study

For the equilibrium study, experiments were carried out in the time established in the kinetic study, being subsequently applied the adsorption isotherm models of Langmuir (Langmuir, 1918) (Eq. (4)), Freundlich (Freundlich, 1906) (Eq. (5)) and Langmuir-Freundlich (Eq. (6)) in order to evaluate the data of the process.

$$q_e = \frac{q_{max} K_L C_e}{1 + K_L C_e} \tag{4}$$

where q_e is adsorptive capacity at the equilibrium corresponding to a C_e, q_{max} is the maximum predicted adsorptive capacity ($mg\ g^{-1}$), K_L represents the affinity between adsorbent and adsorbate ($L\ mg^{-1}$), and C_e is the adsorbate concentration at equilibrium ($mg\ L^{-1}$).

$$q_e = K_F (C_e)^{\frac{1}{n}} \tag{5}$$

where K_F ($L\ g^{-1}$) and n (dimensionless) are model constants; K_F indicate the adsorption capacity of the adsorbent and n indicate the efficiency of the adsorption process.

$$q_e = q_{max} \frac{(K_{LF} C_e)^{\frac{1}{n}}}{1 + (K_{LF} C_e)^{\frac{1}{n}}} \tag{6}$$

where K_{LF} is the affinity constant ($L\ mg^{-1}$).

According to Freundlich (1906), for the values of constant n between 1 and 10, the adsorption is considered favourable. For Langmuir, a dimensionless (R_L) can relate essential characteristics in terms of a separation factor, which enables to predict the form of the adsorption isotherm, indicating whether the adsorption process is favourable or not (Sekar et al., 2004). The process is considered unfavourable when $R_L > 1$, linear when $R_L = 1$, favourable in the interval $0 < R_L < 1$ and irreversible when $R_L = 0$ (El Haddad et al., 2014). The separation factor (R_L) can be calculated as indicated in Eq. (7).

$$R_L = \frac{1}{1 + bC_0} \tag{7}$$

where b is calculated according to Eq. (8).

$$b = \frac{K_L}{q_e} \tag{8}$$

The software used to adjust kinetic and equilibrium models to the experimental data was Origin 8.0, through non-linear regressions. The models plotting was evaluated by the relative standard deviations (S_R^2) and the coefficients of regression (R^2). To evaluate the models that were more suitable to the experimental data, the F Test was used (Montgomery, 2012). F_{calc} is defined by Eq. (9).

$$F_{cal} = \frac{S_R^2(A)}{S_R^2(B)} \tag{9}$$

where $S_R{}^2(A)$ and $S_R{}^2(B)$ are the model's standard deviations, and $S_R(A) > S_R(B)$. If $F_{cal} > F_{tab}$, the model B present a better adjustment in relation to the model A with a 95% of confidence level. However, if $F_{cal} \leq F_{tab}$, the models do not present significant statistically differences.

2.6. Thermodynamic study

The thermodynamic parameters, such as Gibbs free energy ($\Delta G°$), enthalpy ($\Delta H°$) and entropy ($\Delta S°$) were evaluated from the adsorption isotherms. Gibbs free energy ($\Delta G°$) was calculated from the equilibrium constant (K_e) ($L\ g^{-1}$), as shown in Eqs. (10) and (11).

$$K_e = \frac{q_e}{C_e} \tag{10}$$

$$\Delta G\hat{A}^\circ = -RT \ln K_e \tag{11}$$

where R is the universal gas constant and T is the absolute temperature (K).

Gibbs free energy reflects the spontaneity of the process; if it is positive ($\Delta G° > 0$), the process is non-spontaneous and, if negative ($\Delta G° < 0$), it is spontaneous. From the graph of $\Delta G°$ and its respective gradients, were calculated $\Delta H°$ and $\Delta S°$, through Eq. (12).

$$\Delta G\hat{A}^\circ = \Delta H\hat{A}^\circ - T\Delta S\hat{A}^\circ \tag{12}$$

3. Results and discussion

This study was aimed at analysing the interaction between orange albedo and a cationic dye, using MB as a reference, characterising the process in terms of the variation of pH, temperature, stirring rate, dye concentration and influence of salinity (ionic strength).

3.1. Characterisation of citric albedo

In Fig. 1 are presented the micrographs obtained in a scanning electron microscope (SEM) at the different amplitudes of albedo.

The morphology presented by the SEM for albedo indicated a high degree of roughness and waviness, as well as porous and finely segregated particles, indicating a favorable adsorption process. For Weber et al. (2013), such features may favour the diffusion and adsorption of dye molecules into the internal space of the biomass.

Fig. 2 presents the spectra of the adsorbent (biosorbent) measured in the region from 400 to 3,500 cm^{-1}, that indicated the presence of weak vibrations in the region of 3,500–400 cm^{-1}, suggesting the presence of several functional groups.

The band located in the spectrum 3273 cm^{-1} is characteristic of the vibrational stretching of —OH (Abdelwahab et al., 2015), while the band located at 2918 cm^{-1} is associated to vibrational elongation of the C—H (Angin, 2014) and the spectrum located at 2385 cm^{-1} is the band of $CH/CH_2/CH_3$, correspondent to asymmetric C—H vibration and the symmetric stretching vibration of —CH_2— groups. The band located at 1700 cm^{-1} is assigned to the carbonyl (—C═O) stretching from the carboxylic acid (COOH), and the spectra between 1,100 and 990 cm^{-1} includes all the vibrations from the —C═O bonds in the primary and secondary hydroxyl and the carboxylic acid (Lugo-Lugo et al., 2012). These peaks indicate that the biomass has ionizable functional groups (hydroxyl, carbonyl and carboxylic) that favors the sorption of cationic adsorbates such as MB. Montanher et al. (2007) and Boniolo et al. (2010) also reported that the most significant functional groups in the FTIR spectrum of albedo are associated with fibres and carbohydrates, typically found in citrus residues, which favour the adsorption process.

Fig. 1. Scanning electron microscopy with magnifications of 100x (A), 300x (B) and 700x (C).

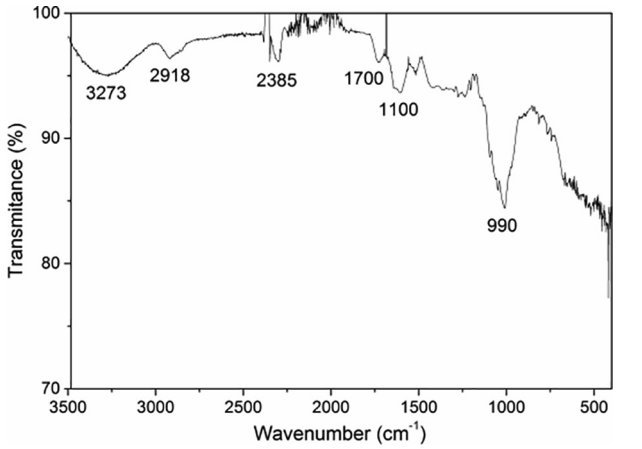

Fig. 2. Fourier transform infrared spectra of albedo.

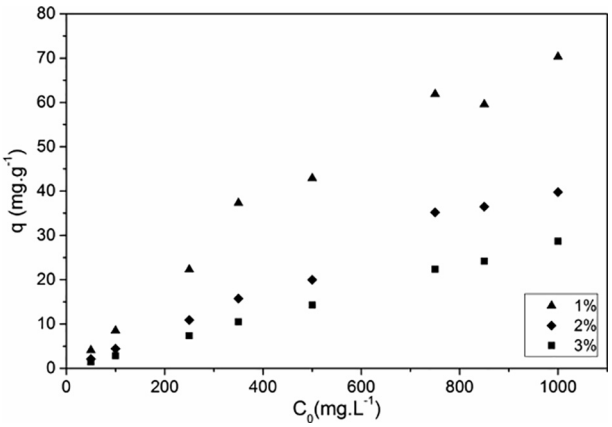

Fig. 3. Influence of biomass dosage. Experimental conditions: C_0 = 50–1000 mg L^{-1}, rotation = 100 rpm, time = 60 min and T = 30 °C.

The point of zero charge for determining the surface charge of albedo was of 4.61 (Silva et al., 2016). The adsorption of cations is favoured when the pH of the solution is greater than the pH_Z, while the adsorption of anions is favoured at a pH lower than the pH_Z (Srivasta et al., 2008). Thus, the adsorption of MB is promoted at pH values higher than the pH_Z. The result was similar to the one found by Montanher et al. (2007), Clemente et al. (2012) and Tozatti et al. (2013), who obtained values pH_Z for orange residue of 4.25, 4.44 and 4.38, respectively.

3.2. Effect of dye solution pH, biomass load and rotation

In order to verify whether the pH of the solution would vary over time with the increase on concentration levels, a study was carried out using dye solutions at the concentration levels of 50–1,000 mg L^{-1} at natural pH, as shown in **Fig. S1 (Supplementary Information - SI)**. The result indicated no significant change of the pH of the solutions over time, verifying the stability of the adsorption process.

The influence of biomass load was evaluated aiming at the optimum relation between mass of adsorbent and adsorbate concentration (Fig. 3). A higher adsorptive capacity (q) can be observed for a lower ratio of adsorbent/adsorbate (1%), while a reduction of q is seen with an increase of adsorbent mass, due to this higher ratio (w/v).

Fig. 4 illustrates the study regarding the influence of stirring rate on the adsorptive capacity, with rotation varying in 60, 80 and 100 rpm. With this, an increase on the adsorptive capacity (q) was observed with an increase on the stirring rate from 60 to 100 rpm. Schimpf et al. (2007) considered that this phenomenon possibly occurred due to the fact that the mass transfer is negligible when the stirring rate is not sufficient to minimise the width of the boundary layer that involves the particle of the solid.

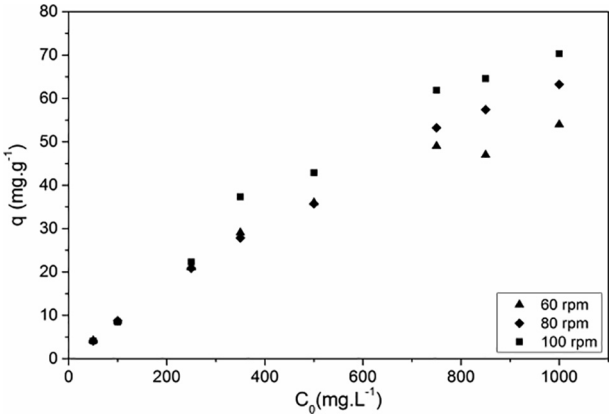

Fig. 4. Influence of rotation on the removal of MB from orange albedo. Experimental conditions: C_0 = 100 mg L^{-1}, time = 60 min, biomass dosage = 1% (w/v) and T = 30 °C.

3.3. Kinetic study

These studies were carried out based on the best results obtained on the study of pH effect (natural pH of the solution), biomass dosage (1% w/v) and stirring rate/rotation (100 rpm). Fig. 5 shows the kinetic evolution curves for dye concentration levels ranging from 50 to 1,000 mg L^{-1} at the times of 0 to 60 min.

It was observed that the adsorption of dye increases rapidly in the initial adsorption times (until 5 min), reducing the adsorption velocity near the equilibrium (10 min) for concentration levels higher than 100 mg L^{-1}.

Fig. 6 illustrates the kinetic evolution curve for the adsorption of MB at concentration levels of 50, 100, 250, 500, 750 and 1,000 mg L^{-1} and the non-linear adjustment to the pseudo-first and pseudo-second order kinetic models.

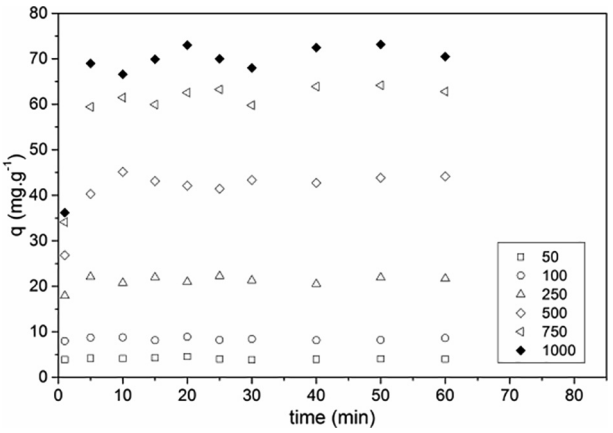

Fig. 5. Kinetic evolution of MB at different dye concentrations. Experimental conditions: biomass dosage = 1% (w/v), rotation = 100 rpm and T = 30 °C.

The initial concentration is an important parameter to surpass all mass transfer resistance between the aqueous and solid phases. At low concentration levels, the proportion of active sites and dye molecules can be high and, thus, all molecules can interact with the adsorbent and be removed from the solution almost immediately. The development of the kinetic models of adsorption is based, mainly, on the fundamental approach of interfacial kinetics and its modifications. Both kinetic models were used to adjust the experimental data, the pseudo-first and pseudo-second order models, for different initial concentrations.

Table 1 presents the values of the correlation coefficients (R^2) obtained from the adjustment to the experimental data using the kinetic models studied. The values of R^2 for the pseudo-first order model are seen as relatively close to the ones obtained for the pseudo-second order model.

The results indicated that $F_{cal} > F_{tab}$ (3.18), at a confidence level of 95%, suggesting a significant difference between both models. Although the models presented good adjustments to the experimental data, the pseudo-first order model exhibited a more adequate adjustment, given the lower residuals (S_R^2) at all concentrations studied.

The pseudo-first-order model relates the removal rate of adsorption directly to the difference in saturation concentration and the number of adsorbent active sites, whereas the pseudo-second order model relates the reaction rate with the amount of solute adsorbed on the surface and at equilibrium of the adsorbent (Ho, 2006). Similar result was obtained by Pavan et al. (2008) using passion fruit peel for removal of MB. According to the authors the best fit to the pseudo-first order model indicates ionic exchange in the adsorptive process.

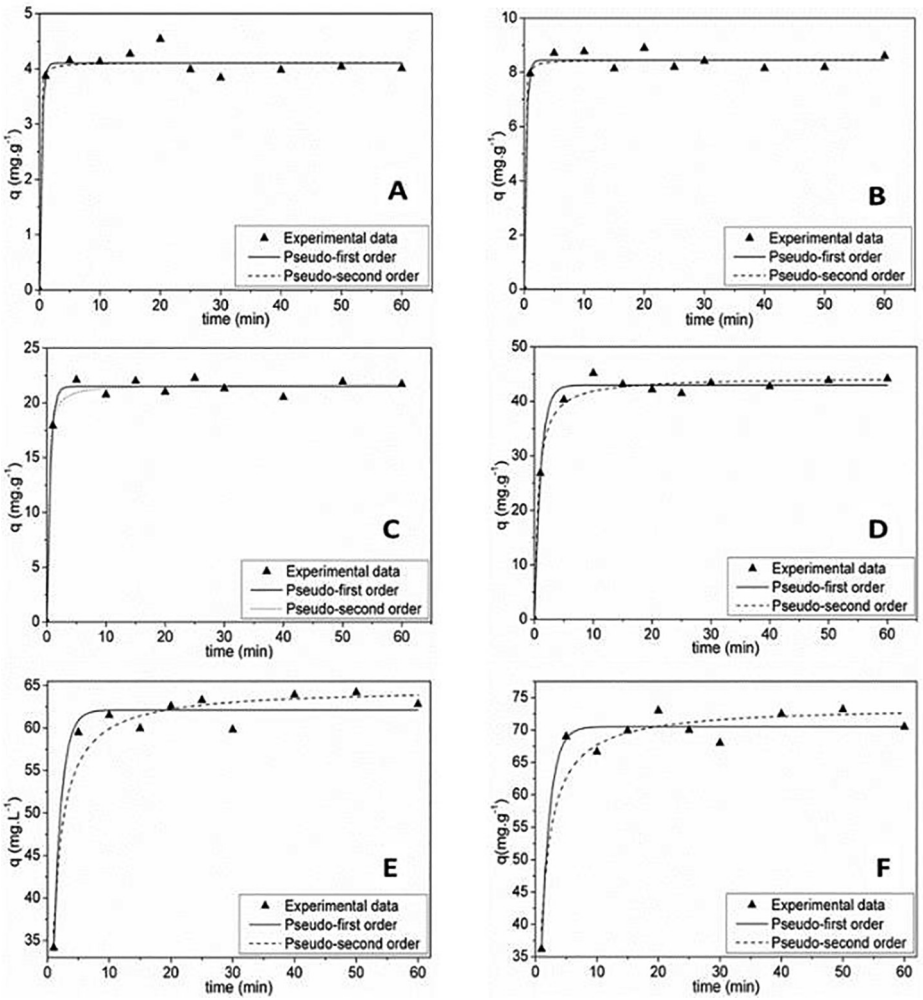

Fig. 6. Kinetic evolution of the adsorption of MB and the non-linear adjustment to the kinetic models, for (a) 50 mg L^{-1}, (b) 100 mg L^{-1}, (c) 250 mg L^{-1}, (d) 500 mg L^{-1}, (e) 750 mg L^{-1} and (f) 1,000 mg L^{-1}.

Table 1
Parameters of the kinetic models for the analysis of orange albedo.

Models	Parameters	Concentrations (mg L^{-1})					
		50	100	250	500	750	1000
Pseudo-first order (1)	q_{calc} (mg g^{-1})	4.11	8.45	21.51	42.97	62.10	70.51
	k_1 (min^{-1})	2.86	2.84	1.79	0.96	0.79	0.72
	S_R^2	0.33	0.72	3.25	15.57	22.05	38.90
	R^2	0.98	0.99	0.99	0.99	0.97	0.96
Pseudo-second order (2)	q_{calc} (mg g^{-1})	4.11	8.47	21.74	44.40	64.72	73.70
	k_2 (g mg^{-1} min^{-1})	4.53	2.23	0.23	0.04	0.019	0.015
	S_R^2	0.34	0.78	4.26	17.73	33.89	75.83
	R^2	0.97	0.99	0.99	0.99	0.95	0.92
***F* Test**	F_{cal} (2/1)	1.03	1.08	1.31	1.14	1.53	1.95
	F_{tab}	**3.18**					

3.4. Equilibrium study

The adsorption isotherms describe how the adsorbate interacts with the adsorbent, enabling to predict the mechanism and nature of the interaction (Ahmed and Theydan, 2012). The adsorption isotherms at the temperatures of 30, 45 and 60 °C are presented in Fig. 7. Table 2 presents the parameters obtained from the adjustments of the Langmuir, Freundlich and Langmuir-Freundlich models for the removal of methylene blue.

By analysing the table, it can be observed that the results obtained for the *F*-Test do not present any significant difference between the three models for the isotherm at 60 °C, as well as between the Langmuir and Langmuir-Freundlich for the isotherms at 30 and 45 °C, for $F_{cal} < F_{tab}$ (3.79), at a confidence level of 95%. However, the Freundlich model presented a significant difference when compared to the other models for the temperatures of 30 and 45 °C.

The values of the constant *n* lie between 1 and 10, indicating that the adsorption process of dye is favourable for the adsorbent originated from orange albedo. Despite the fact that the high values of *K* and *n* indicate high adsorption in the Freundlich model, the correlation coefficient (R^2 = 0.94–0.95) was the lowest among the models evaluated at both temperatures.

The Langmuir-Freundlich model, also called the Sips model, presents the combination of the Langmuir and Freundlich equations, generally obtaining a better fit in a heterogeneous surface adsorbent. The difference between this equation and that of Langmuir is the additional parameter of 1/n, characterizing the heterogeneity of the system, so larger this parameter, more heterogeneous the system is (Húmpola et al., 2013).

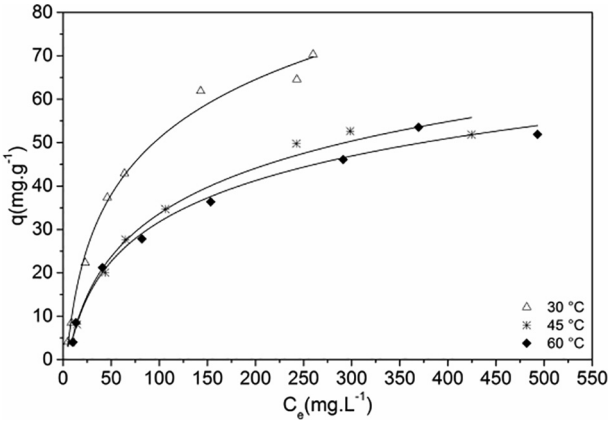

Fig. 7. Adsorption isotherms at the temperatures of 30, 45 and 60 °C for orange albedo. Experimental conditions: biomass dosage = 1%, rotation = 100 rpm and time = 20 min.

Still, according to Table 2, smaller residue (SR^2) of the Sips model is observed, indicating a better fit of this model to the experimental data. Similar results were obtained by Pavan et al. (2008) and Balarak et al. (2015) who used passion fruit peel and canola residues, respectively, to remove MB, obtaining lower SR^2 for the Langmuir-Freundlich (Sips) model.

The isotherms obtained for the stirring rates of 60 and 80 rpm are presented on Fig. S2 and S3 and its respective adjustments in Table S1 (SI). The values of R_L for the isotherms at the rotation of 100 rpm are presented in Table 3. According to the results obtained, R_L stands between 0 and 1, indicating a favourable adsorption for all parameters evaluated (concentration and stirring rate); for 80 and 60 rpm, the values of R_L are exhibited in Table S2 (SI).

Table 4 compares the adsorptive capacity of the biomass used in this study with the other biomass types reported in the literature for the adsorption of dyes, being relevant to highlight the potential of orange albedo in comparison with the other several lignocellulosic residues.

3.5. Thermodynamic study

The effect of the temperature in the experiences of dye adsorption was investigated at three different temperatures (30, 45 and 60 °C) and three evaluated rotations (60, 80 and 100 rpm), making it possible to observe a higher adsorptive capacity for a rotation of 100 rpm.

The results indicated that the increase in temperature negatively influenced the adsorption of dye, representing an exothermic adsorption. According to Abdelwahab et al. (2015), the reduction on adsorption with the increase in temperature can be due to the weaker adsorption forces between the active sites of the adsorbent and the molecules of adsorbate.

The value of the thermodynamic parameters ($\Delta G°$, $\Delta H°$ e $\Delta S°$) obtained from the values of C_e and q_e (Fig. 7) are presented in Table 5. From the graph of $\Delta G°$ (kJ mol^{-1}) vs. temperature (K), presented in Fig. 8, it was possible to obtain the values of $\Delta H°$ and $\Delta S°$, through the linear and angular coefficient, respectively.

The negative value of ΔH indicated that the process is of exothermic nature. Thus, the energy absorbed in breaking the bond is lower than the energy released in the bond formations, releasing energy in the form of heat. The negative value of ΔS suggests a reduction of the randomness of the interface solid/solution, with no significant changes in the internal structure of the adsorbents through adsorption (Mohan and Singh, 2002; Alkan et al., 2007). The thermodynamic parameters for the rotations of 60 and 80 rpm are presented in Table S3 (SI).

Similar behavior was observed by Miraboutalebi et al. (2017) who used maize silk as adsorbent to remove MB obtaining negative values for thermodynamic parameters.

Table 2
Parameters for the equilibrium models at the temepratures of 30, 40 and 60 °C for orange albedo.

Models	Parameters	Temperature (°C)		
		30	45	60
Langmuir (1)	q_{calc} (mg g^{-1})	85.74	67.12	63.70
	K_L (L mg^{-1})	0.015	0.01	0.01
	S_R^2	29.52	18.05	32.27
	R^2	0.99	0.99	0.99
Freundlich (2)	K_F (L g^{-1})	5.54	3.74	3.65
	n	2.16	2.20	2.26
	S_R^2	234.10	143.94	101.28
	R^2	0.94	0.94	0.95
Langmuir-Freundlich (3)	q_{calc} (mg g^{-1})	77.79	61.27	67.54
	K_{LF} (L mg^{-1})	0.009	0.005	0.01
	n	0.836	0.85	1.09
	S_R^2	18.02	12.39	30.78
	R^2	0.99	0.99	0.98
***F* Test**	F_{cal} (1/2)	7.90	7.97	3.14
	F_{cal} (1/3)	1.64	1.46	1.05
	F_{cal} (2/3)	12.99	11.62	3.29
	F_{tab}	**3.79**		

Table 3
The values of R_L for the isotherms at the temperatures of 30, 40 and 60 °C for orange albedo.

T (°C)	C_0 (mg L^{-1})							
	50	100	250	350	500	750	850	1000
30	0.845	0.850	0.856	0.877	0.851	0.846	0.835	0.824
45	0.890	0.891	0.889	0.888	0.874	0.869	0.861	0.838
60	0.889	0.895	0.895	0.888	0.879	0.860	0.863	0.838

Table 4
Experimental adsorptive capacity (mg g^{-1}) for the several types of dyes using low-cost adsorbents (biosorbents) **without any activation process**.

Biomass	Dye	q_e (mg g^{-1})	Reference
Passion fruit	Methylene Blue	44.70	Pavan et al. 2008
Mango seed	Methylene Blue	25.36	Kumar et al., 2012
Coconut fibre	Methylene Blue	29.50	Etim et al. 2016
Potato skin	Methylene Blue	52.60	Gupta et al. 2016
Potato skin	Malachite green	33.30	Gupta et al. 2016
Orange albedo	Methylene blue	70.30*	This study

* 30 °C, 100 rpm, 1% of albedo (w/v) for 20 min.

Table 5
Thermodynamic parameters for the interaction between the dye and orange albedo.

Temperature (K)	Thermodynamic parameters		
	ΔG (kJ mol^{-1})	ΔS (kJ mol^{-1})	ΔH (kJ mol^{-1})
303.15	−14.26	−0.0228	−21.19
318.15	−13.92		
333.15	−13.58		

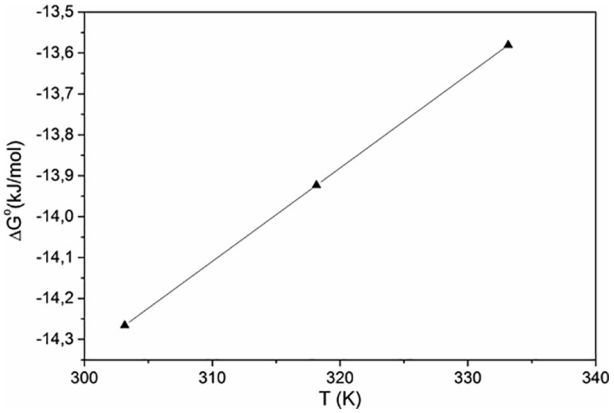

Fig. 8. Variation of Gibbs free energy with temperature.

3.6. Ionic strength (Salinity)

The influence of salinity on the process of adsorption is considered of relevant importance, given the presence of fixed solids in industrial effluents (Silva et al., 2016), which may interfere on the adsorption of cationic dyes as a result of two different mechanisms: (1) competition between the cationic ions (in this case, Na^+), reducing the electrostatic potential on the surface; (2) increased ionic strength, compressing the double electric layer and leading to electrostatic repulsion of the cationic dye from the surface (Punjongharn et al., 2008; Weng et al., 2009).

Fig 9 illustrates the great influence of salt concentration on the adsorptive capacity, reducing concentrations in 20–65% when reaching 10 g L^{-1} of salt. Textile effluents usually display total solid content values in the range 1,000–1,600 mg L^{-1}; however, this reference value may vary depending on the process and type of water used, also as a possible result of pH adjustment (Braile and Cavalcanti, 1979, Silva et al., 2016). It was verified by Silva et al. (2016) that of the 3.4 g L^{-1} of total solids, approximately 1.2 g L^{-1} were total fixed solids in real textile effluent, representing essentially salts and oxides. Thus, roughly 50% of the effluent will have to be diluted in order to obtain a higher COD and colour removal, justifying water recycling, given the high removal capacity, as well as safeguarding the sustainability of the process. With a concentration of 1 g L^{-1} of NaCl, there was an efficiency loss between 10 and 15% in this work.

Dried seagrape used in the removal of cationic dyes obtained a reduction of>50% on the adsorption capacity when NaCl concentration shifted between 0 and 10 g L^{-1} in solution (Punjongharn et al., 2008). The removal of MB using hazelnut shell resulted in the

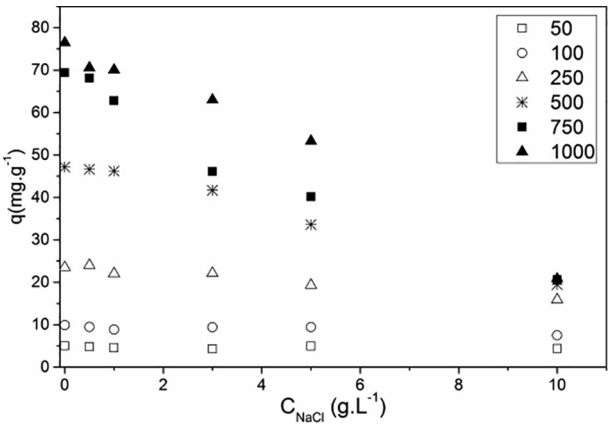

Fig. 9. Adsorption capacity *versus* NaCl concentration. Experimental conditions: biomass dosage = 1% (w/v), rotation = 100 rpm and time = 20 min.

reduction of 23% on the adsorption capacity of the dye when subject to a concentration of 5 g L^{-1} of NaCl (Dogan et al., 2009). Weng et al. (2009), using pineapple waste, verified a reduction of up to 18% on the removal capacity of MB using $NaNO_3$ in a solution with concentration levels between 0.425 and 5.95 g L^{-1}.

4. Conclusions

Orange albedo is indeed a viable residue to be used as adsorbent for the removal of MB. The residue exhibited characteristics such as porosity, functional groups and surface charge which can optimise the adsorption capacity of cationic compounds. In the kinetic study, there was no significant difference observed between the models. As for the equilibrium study, the Langmuir-Freundlich model was found to best represent the system. The thermodynamic parameters demonstrated that the process is viable, given the spontaneous and exothermic nature of the process. The value of ΔS° suggests a reduction on the disorder on the interface solid/-solution throughout the adsorption of MB dye in orange albedo. The results demonstrated the capacity of the adsorbent for the removal of MB.

Acknowledgements

The authors thank CNPq – Brazil - Process number 249182/2013-0, for resources and fellowship.

Conflict of interest statement

Authors declare that there is no conflict of interest.

Appendix A. Supplementary material

Supplementary data to this article can be found online at https://doi.org/10.1016/j.jksues.2019.04.006.

References

Abdelwahab, O., Fouad, Y.O., Amin, N.K., Mandor, H., 2015. Kinetic and thermodynamic aspects of cadmium adsorption onto raw and activated guava (*Psidium guajava*) leaves. Environ. Prog. Sustain. 34, 351–358.
ABF, 2013. Anuário Brasileiro da Fruticultura. Gazeta Santa Cruz, Santa Cruz do Sul, Brazil, (acessed 10 November 2014). <http://www.grupogaz.com.br/editora/anuarios/lista_categoria/cat:4>.
Ahmed, J.M., Theydan, K.S., 2012. Equilibrium isotherms, kinetics and thermodynamics studies of phenolic compounds adsorption on palm-tree fruit stones. Ecotox Environ. Safe 84, 39–45.
Aksu, Z., 2005. Application of biosorption for the removal of organic pollutants: a review. Process Biochem 40, 997–1026.
Alkan, M., Demirbas, O., Dogan, M., 2007. Adsorption kinetics and thermodynamics of an anionic dye onto sepiolite. Micropor. Mesopor. Mat. 101, 388–396.
Angin, D., 2014. Utilization of activated carbon produced from fruit juice industry solid waste for the adsorption of Yellow 18 from aqueous solutions. Bioresour. Technol. 168, 259–266.
Asgher, M., Bhatti, H.N., 2012. Evaluation of thermodynamics and effect of chemical treatments on sorption potential of citrus waste biomass for removal of anionic dyes from aqueous solutions. Ecol. Eng. 38, 79–85.
Babbar, N., Oberoi, H.S., 2014. Enzymes in value-addition of agricultural and agro-industrial residues. Enzymes Value-Addition Wastes 2, 29–50.
Balarak, D., Jaafari, J., Hassani, G., Mahdavi, Y., Tyagi, I., Agarwal, S., Gupta, V.K., 2015. The use of low-cost adsorbent (Canola residues) for the adsorption of methylene blue from aqueous solution: Isotherm, kinetic and thermodynamic studies. Coll. Interf. Sci. Commun. 7, 16–19.
Boniolo, M.R., Yamaura, M., Monteiro, R.A., 2010. Biomassa residual para remoção de íons uranilo. Quim Nova 33, 547–551.
Braile, P.M., Cavalcanti, J.E.W.A., 1979. Manual de tratamento de águas residuárias industriais. São Paulo, CETESB, 1979, p. 764.
Clemente, E., Flores, A.C., Rosa, C.I.L.F., Oliveira, D.M., 2012. Características da farinha de resíduos do processamento de laranja. R Ciências Exatas e Naturais 14, 257–269.
Daud, Z., Nasir, N., Kadir, A.A., Latiff, A.A.A., Ridzuan, M.B., Awang, H., Halim, A.A., 2018. Potential of agro waste-derived absorbent material for colour removal. Deffect Diffus Forum 382, 292–296.
Dogan, M., Abak, H., Alkan, M., 2009. Adsorption of methylene blue onto hazelnut shell: kinetics, mechanism and activation parameters. J. Hazard Mater. 164, 172–181.
El Haddad, M., Regti, A., Laamari, M.R., Slimani, R., Mamouni, R., Antri, S.E., Lazar, S., 2014. Calcined mussel shells as a new and eco-friendly to remove textile dyes from aqueous solutions. J. Taiwan Inst. Chem. E 45, 533–540.
Etim, U.J., Umoren, S.A., Eduok, U.M., 2016. Coconut coir dust as a low cost adsorbent for the removal of cationic dye from aqueous solution. J. Saudi Chem. Soc. 20, 67–76.
Freundlich, H., 1906. Over the adsorption in solution. J. Phys. Chem. 57, 358–471.
Gupta, N., Kushwaha, A.K., Chattopadhyaya, M.C., 2016. Application of potato (*Solanum tuberosum*) plant wastes for the removal of methylene blue and malachite green dye from aqueous solution. Arab J. Chem. 9, 707–716.
Ho, Y.S., McKay, G., 1998. Kinetic models for the sorption of dye from aqueous solution by wood. Process Saf Environ 76 (May), Part B.
Ho, Y.S., McKay, G., 2000. The kinetics of sorption of divalent metal ions onto sphagnum moss peat. Water Res. 34 (3), 735–742.
Ho, Y.S., 2006. Review of second-order models for adsorption systems. J Hazar. Mater. B 136, 681–689.
Húmpola, P.D., Odetti, H.S., Fertitta, A.E., Vicente, J.L., 2013. Thermodynamic analysis of adsorption models of phenol in liquid phase on different activated carbons. J. Chil. Chem. Soc. 58, 1541–1544.
IBGE, 2018. Instituto Brasileiro de Geografia e Estatística. (acessed 12 Sep 2018), <http://agenciabrasil.ebc.com.br/economia/noticia/2018-09/pais-tem-safra-recorde-de-frutas-cereais-leguminosas-e-oleaginosas>.
Kumar, P.S., Ramalingam, S., Sathyaselvabala, V., Kirupha, S.D., Murugesan, A., Sivanesan, S., 2012. Removal of cadmium(II) from aqueous solution by agricultural waste cashew nut shell. Korean Journal of Chemical Engineering 29, 756–768.
Kumar, P.S., Palaniyappan, M., Priyadharshini, M., Vignesh, A.M., Thanjiappan, A., Fernando, P.S.A., Ahmed, R.T., Srinatha, R., 2014. Adsorption of basic dye onto raw and surface-modified agricultural waste. Environ. Prog. Sustain 33, 87–98.
Langmuir, I., 1918. The adsorption of gases on plane surfaces of glass, mica and platinum. J. Am. Chem. Soc. 40, 1361–1403. https://doi.org/10.1021/ja02242a004.
Liu, T., Li, Y., Du, Q., Sun, J., Jiao, Y., Yanga, G., Wanga, Z., Xia, Y., Zhang, W., Wang, K., Zhu, H., Wu, D., 2012. Adsorption of methylene blue from aqueous solution by graphene. Coll. Surf. B: Biointerf. 90, 197–203.
Lugo-Lugo, V., Barrera-Díaz, C., Ureña-Nüñez, F., Bilyeu, B., Limares-Hernández, I., 2012. Biosorption of Cr(III) and Fe(III) in single and binary systems onto pretreated orange peel. J. Environ. Manage. 112, 120–127.
Mckay, G., Otterburn, M.S., Sweeney, A.G., 1980. The removal of colour from effluent using various adsorbents-III, silica: rate processes. Water Res. 14, 15–20.
Miraboutalebi, S.M., Nikouzad, S.K., Peydayesh, M., Allahgholi, N., Vafajoo, L., McKay, G., 2017. Methylene blue adsorption via maize silk powder: Kinetic, equilibrium, thermodynamic studies and residual error analysis. Process Saf. Environ. 106, 191–202.
Mohan, D., Singh, K.P., 2002. Single and multi-component adsorption of cadmium and zinc using activated carbon derived from bagasse - an agricultural waste. Water Res. 36, 2304–2318.
Montanher, S.F., Oliveira, E.A., Rollemberg, M.C., 2007. Utilization of agro-residues in the metal ions removal from aqueous solutions. Hazard. Mater. Wastewater: Treat. Removal Anal. 1, 51–78.
Montgomery D.C., Introdução ao controle estatístico da qualidade, 4 ed., LTC, 2012.
Moubarak, F., Atmani, R., Maghri, I., Elkouali, M., Talbi, M., Latifa, M., 2014. Elimination of methylene blue dye with natural adsorbent "banana peels powder". Global J. Sci. Front. Res. 14, 39–44.
Najafi, H., Pajootan, E., Ebrahimi, A., Arami, M., 2016. The potential application of tomato seeds as low-cost industrial waste in the adsorption of organic dye molecules from colored effluents. Desalin. Water Treat. 57, 15026–15036.

Pavan, F.A., Lima, E.C., Dias, S.L.P., Mazzocato, A.C., 2008. Methylene blue biosorption from aqueous solutions by yellow passion fruit waste. J. Hazard Mater. 150, 703–712.

Punjongharn, P., Meevasana, K., Pavasant, P., 2008. Influence of particle size and salinity on adsorption of basic dyes by agricultural waste: dried Seagrape (*Caulerpa lentillifera*). J. Environ. Sci. 20, 760–768.

Saini, J., Garg, V.K., Gupta, R.K., 2018. Removal of methylene blue from aqueous solution by Fe_3O_4@Ag/SiO_2 nanospheres: synthesis, characterization and adsorption performance. J. Mol. Liq. 250, 413–422.

Schimpf, S., Louis, C., Claus, P., 2007. Ni/SiO_2 catalysts prepared with ethylenediamine nickel precursors: Influence of the pretreatment on the catalytic properties in glucose hydrogenation. Appl. Catal. A-Gen 318, 45–53.

Sekar, M., Sakthi, V., Rengaraj, S., 2004. Kinetics and equilibrium adsorption study of lead (II) onto activated carbon prepared from coconut shell. Coll. Interf. Sci. 279, 307–313.

Sharma, K., Mahato, N., Cho, M.H., Lee, Y.R., 2017. Converting citrus wastes into value added products: economical and environment friendly approaches. Nutrition 34, 29–46.

Sharma, N., Tiwari, D.P., Singh, S.K., 2014. The efficiency appraisal for removal of Malachite Green by potato peel and neem bark: isotherm and kinetic studies. Int. J. Chem. Environ. Eng. 5, 84–88.

Silva, C.E.F., Gonçalves, A.H.S., Abud, A.K.S., 2016. Treatment of textile industry effluents using orange waste: a proposal to reduce color and chemical oxygen demand. Water Sci. Technol. 74, 994–1004.

Srivasta, V.C., Mall, I.D., Mishra, I.M., 2008. Adsorption of toxic metal ions onto activated carbon. study of sorption behaviour through characterization and kinetics. Chem. Eng. Proc. 47, 1269–1280.

Tozatti, P., Rigo, M., Bezerra, J.R.M.V., Cordova, K.R.V., Teixeira, A.M., 2013. Utilização de resíduo de laranja na elaboração de biscoitos tipo cracker. R de Ciências Exatas e Naturais 15, 135–150.

Wang, Y., Zhang, Y., Li, S., Zhong, W., Wei, W., 2018. Enhanced methylene blue adsorption onto activated reed-derived biochar by tannic acid. J. Mol. Liq. 268, 658–666.

Weber, C.T., Foletto, E.L., Meili, L., 2013. Removal of tannery dye from aqueous solution using papaya seed as an efficient natural biosorbent. Water Air Soil Poll. 224, 1427–1438.

Weng, C.H., Lin, Y.T., Tzeng, T.W., 2009. Removal of methylene blue from aqueous solution by adsorption onto pineapple leaf powder. J Hazard. Mater. 170, 417–424.

Yagub, M.T., Sen, T.K., Ang, H.M., 2012. Equilibrium, kinetics, and thermodynamics of methylene blue adsorption by pine tree leaves. Water Air. Soil Pollut. 223, 5267–5282.

Zema, D.A., Calabrò, P.S., Folino, A., Tamburino, V., Zappia, C., Zimbone, S.M., 2018. Valorisation of citrus processing waste: a review. Waste Manage 80, 252–273.

Zhao, X., Liu, W., Deng, Y., Zhu, J.Y., 2017. Low-temperature microbial and direct conversion of lignocellulosic biomass to electricity: advances and challenges. Renew. Sust. Energ. Rev. 71, 268–282.